Coiling in gastropods: a lead to synthesis

Ido Filin [1] *

[1] Kangasala, Finland

* Corresponding author. E-mail: ido@filin.fi

Running headline: Coiling in gastropods.

Supplementary material: SI appendix.

The author(s) declare(s) no conflict of interest.

This manuscript was compiled on 4 January 2026.

DRAFT

Abstract

Biological structures lie at intersections of function, construction and history. Conversely, the geometry of structures modulates how these three aspects of organic form manifest in different taxonomic groups and ecological circumstances, raising challenges to causal inferences. Here, I apply the familiar logarithmic helicospiral (logspiral) model for coiled shells, to assess its fit to data on gastropods, and to study allometry, covariation and constraint in coiling behavior, in light of adaptationist and proximate mechanistic explanations. I derive convenient expressions for the three-way relationship between expansion rate, apical angle and downward lead angle of spiral paths on shells. Combining several published datasets, I find that centerline spirals of gastropod shells follow isometrically growing conical logspirals. Allometry manifests in the relative growth of apertures. Both empirical patterns and theoretical arguments further suggest that the relation between apical angle and expansion rate, usually attributed to economical and mechanical demands, can equally be explained by taxon-specific lead angles and plasticity in growth. Consequently, the lead angle emerges as a more biologically meaningful coiling parameter. I relate results to the longstanding methodological problem of confusing spire-height allometry with incorrect longitudinal origin of measurement, and to empirically derived patterns of covariation of coiling parameters and morphometric traits in gastropods. More generally, I demonstrate dangers of relying on only single methods, or on generic formulas and workflows, and that geometry dictates particular "laws of form" that have practical use in data analyses and integration, and need to be fully acknowledged when seeking causal adaptationist or mechanistic explanations.

Keywords: allometry, morphometrics, ontogeny, conchology, developmental plasticity, theoretical morphology, mollusc, molluscan shell

DRAFT

Introduction

Since antiquity, molluscan shells have served as exemplars for the immense variety of nature and, in the past two centuries, to how such diversity can be understood and unified by mathematical modeling (Moseley 1838, 1842, Thompson [1942] 1992, Raup 1961, 1966, Vermeij 1993, Stone 1996, McGhee 1999, Urdy 2015, Hammer 2016). Conchiferans also feature prominently in discussions of adaptation and constraint, the exchange among functional, constructional and historical aspects of form that is at the core of biology (Seilacher 1973, Savazzi 1990, Vermeij 1993, Edie et al. 2024). The standard point of departure for modeling coiled shelly forms, both extant and fossil, is the logarithmic helicospiral, hereafter, *logspiral* (Thompson [1942] 1992, Raup 1961, 1966, McGhee 1999). Logspirals are famously self-similar, maintaining fixed proportions while expanding in size (i.e., isometric growth). Much literature discusses its inadequacy, due to commonly observed ontogenetic allometry (variation in coiling parameters with age or size) and irregular coiling, where even the coiling axis is not fixed, often associated with important life-history transitions (McGhee 1980, 1999, 2001, Okamoto 1988, Vermeij 1993, Savazzi 1990, 1996, Aldridge 1998, van Osselaer & Grosjean 2000, Liew et al. 2014, Chirat et al. 2021, Ohta et al. 2025).

Nonetheless, logspirals are still widely used in shell modeling (Noshita et al. 2012, Larsson et al. 2020, Chirat et al. 2021, Araki & Noshita 2023), and for good reason. Beyond the mathematical elegance, the conical logspiral can be thought of as a null model for coiled geometries. From principles of relative growth (Huxley [1932] 1993), of multivariate allometry (Klingenberg 1996), and of symmetry (Bookstein 1978, Okamoto 1988), the conical logspiral provides the isometric baseline, against which the nature and magnitude of the inevitable allometry of real shells can be measured.

A first goal of this work, then, is to assess the nature and magnitude of deviations from isometric growth in gastropod shells, by fitting conical logspirals (Fig. 1A,B) to available data. One convenient formulation that explicitly accounts for allometry is

$$r = r(\theta) = r_0 e^{\gamma\theta}, \quad z(r) = T r^k, \qquad [1]$$

where r, θ and z define a cylindrical coordinate system, whose origin is at the apex (or pole) of the helicospiral (Fig. 1A,B). (I note that this allometric logarithmic helicospiral has been derived many times before; though, seemingly, authors were often unaware of earlier formulations; Bayer 1978, Cortie 1989, Schindel 1990, Savazzi 1990, Fowler et al. 1992, Stone 1995, Prusinkiewicz & Fowler 2009, Tursch 1997, van Osselaer & Grosjean 2000, Urdy et al. 2010, Swan 2015, Larsson et al. 2020.)

The z-direction defines the coiling axis of the helicospiral. I will often refer to it as *longitudinal*, and to the value of the z-coordinate as *spire height*. Eq.[1] states that the radius of the spiral, r, expands exponentially at a rate γ, as revolution angle, θ, increases. Spire height, similarly, grows exponentially at a rate γk, where k is the allometric exponent, $k = 1$ being isometric growth. The allometric case, $k \neq 1$, is often called *extraconical* (Raup 1966, van Osselaer & Grosjean 2000) because isometric logarithmic helicospirals are conical (Fig. 1B). Clearly, the isometrically growing conical logspiral is a special case of Eq.[1], where the allometric relation $z(r)$ reduces to simple proportionality. The proportionality constant, T, then, becomes Raup's dimensionless *translation* parameter (Raup 1966), related to β, the half-apical angle of the conical spiral, hereafter *apical angle*, by $T = \cot \beta$ (Fig. 1B).

A shell, however, is not a single helicospiral, but a three-dimensional structure made of "a bunch" of such spirals — hereafter, *multispiral* approach (Fig. 1D; also called multivector; Thompson [1942] 1992, Bayer 1978, McGhee 1999). Alternatively, a shell can be described by a *generating curve*, a closed figure that sweeps through space along a spiral *centerline* (Fig. 1C; Thompson [1942] 1992, Raup 1961, 1966, Okamoto 1988; roughly corresponding to the "ontogeny axis" of Liew & Schilthuizen 2016, and the "internal spiral" of Larsson et al. 2020.) Following Raup (1966), Schindel (1990), van Osselaer & Grosjean (2000) and Larsson et al. (2020), I distinguish among radial expansion of the centerline spiral (r in Eq.[1]; at a rate γ), longitudinal expansion (z in Eq.[1]; at a rate γk), and whorl expansion — expansion of the generating curve, or aperture, itself, to which Raup's *whorl expansion rate*, W, refers, in a strict sense. Denoting allometry of aperture (linear) size by k_w, aperture area, A, grows as $A(\theta) = A_0 e^{2(\gamma k_w)\theta}$ (factor of 2 because A describes area; compare also with Larsson et al.

2020). Exponential expansion of the aperture is, then, at a rate γk_w, and Raup's whorl expansion rate parameter becomes $W = e^{2\pi\gamma k_w}$.

In the isometric case, all three rates are equal ($k = k_w = 1$), and all logspirals on a shell share a single common value of expansion rate (Illert 1983). By geometric necessity, however, they differ in other parameters (Bayer 1978). Particularly, in apical angle, β, and in the downward *lead angle*, λ (Fig. 1B,D,F,G; adopted from the term for the angle of helical threads on a screw). Expansion rate, γ, is typically small (< 0.2) in gastropods (Thompson [1942] 1992, Cameron 1981), because gastropod shells usually exhibit several complete whorls, resulting in the following expression for the three-way covariation of expansion rate, apical angle and lead angle,

$$\tan\lambda \tan\beta = \frac{\gamma}{\sqrt{1+\gamma^2}} \approx \gamma \qquad [2]$$

(note, $\tan\beta = 1/\cot\beta = 1/T$; in the range $\gamma \leq 0.2$, the error of using the approximation, rather than the full expression, is no more than 2%; SI). In the words of D'Arcy Thompson, "It seems a complicated affair; but it is only a pathway winding at a steady slope up a conical hill ... a certain ensemble, or bunch, of these spiral curves in space constitutes the self-similar surface of the shell" (Thompson [1942] 1992). A second goal is to demonstrate how the above expression for this "steady slope" (lead angle, λ) has underappreciated implications to adaptationist and mechanistic interpretation of covariation in coiling parameters in gastropods.

In this paper, I first set to assess to what degree gastropod shells follow logspiral coiling, whose formulation and biological rationale I discussed above. To that end, I examine whether conical envelopes and exponential expansion fit gastropod shells well. As part of this investigation, I revisit the longstanding "pitfall" (van Osselaer & Grosjean 2000) of confounding spire-height allometry with incorrectly accounting for longitudinal origin of measurement. A problem that plagues also modern workflows. I offer a solution, based on fitting nonlinear models. I later provide "materials for a synthesis" (West-Eberhard 2003) that (*i*) reconcile "ideal" logspirals with ontogenetic allometry of "real" shells; (*ii*) discuss implications to mechanistic and adaptationist interpretations of variation in coiling parameters; and (*iii*) tie together disparate results from paleobiology, from different approaches to

theoretical morphology, from empirical studies of intra- and interspecific covariation in morphometric traits, from studies of shell growth at the cellular level, and from observations and experiments of developmental plasticity in gastropods. In pursuing these directions, I am motivated by Raup's (1961, 1966) spirit of practical application and Gould's (1984) pluralistic advocacy for combining "deductive" and "inductive" approaches to shell morphology (more recently, Noshita 2014, Liew & Schilthuizen 2016, and Larsson et al. 2020).

DRAFT

Materials and Methods

Datasets

Data was obtained from tables in Schindel (1990), Dryad repositories for Noshita et al. (2012) and Collins et al. (2021b), and online dataset for Larsson et al. (2020). Datasets from Noshita et al. and Larsson et al. were augmented with additional data from later studies (Araki & Noshita 2023 and Garcia Castillo et al. 2024b, respectively). (Dryad datasets: Noshita et al. 2011 and Collins et al. 2021a; Zenodo dataset: Garcia Castillo et al. 2024a; Other dataset: Larsson & Butlin 2019.)

Data from Schindel and from Noshita et al. contain together estimates of coiling parameters for hundreds of species (and specimens) of marine, freshwater and terrestrial gastropods, such as whorl expansion rate (W; from which γ can be found), apical angle (T, $\cot\beta$), and Schindel's spire expansion rate (equivalent to γk, longitudinal exponential expansion rate; Eq.[1]). Larsson et al.'s data, for intraspecific variation in the intertidal marine snail *Littorina saxatilis*, provides direct estimates of γ and γk, as well as some parameter estimates for centerline spirals and shape and size of apertures (see below).

Collins et al. (2021b) provided a large dataset containing ontogenetic sequences of apertures of fossil and recent marine gastropods of the New Zealand region, obtained from sectioned specimens or microtomography. Their dataset contains both images of sectioned specimens and morphometric measurements of coiling axes, aperture areas, aperture centroids, etc. (Fig. 2). This dataset, therefore, provides an opportunity to directly estimate spiral centerlines (Fig. 1C), and their potential allometry.

For all specimens, from all datasets, additional data, such as species, genus, family, specimen ID, scales of images, etc. were compiled.

Data transformation and reanalysis

Estimated values for W and spire expansion rate from Schindel (1990) were transformed to γ and γk of this study by $\gamma = \frac{\log W}{2\pi}$ and an equivalent expression for spire height (SI). Because estimated parameters in the Noshita et al. dataset refer directly to Raup's model of conical logspiral shells, estimates of k cannot be derived from that data. The expansion rate W was

similarly transformed to γ as above. Values of T in their dataset refer to the logspiral on the aperture margin furthest from the coiling axis. To facilitate comparison with other datasets, these T-values were transformed to roughly represent centerline spirals, by doubling them (more details in SI).

The Larsson et al. dataset provides direct estimates of radial and longitudinal expansion rates, γ and γk. To facilitate comparison with Collins et al., I estimated the centroids of "sectioned" apertures, according to their reported aperture size and shape parameters (see relevant SI section). This reanalysis provided estimates of centerline $\cot\beta$ (i.e., T).

Reanalysis of Collins et al.'s data began by fitting conical envelopes to aperture centroids, i.e., $z(r)$ a linear relationship ($k = 1$ in Eq.[1]), for each specimen, by either linear regression or principal component analysis (PCA; i.e., major-axis type II regression). This procedure located the apex of the enveloping cone, and estimated the apical angle. The reader should note that such an analysis does not mean, in any way, that I claim that the estimated apex is a real feature of the actual shell. Rather, like the coiling axis, the conical envelope "appears *post facto* as a secondarily derived feature of the morphogenetic" processes (Ackerly 1989). For a given specimen, and for the sampled ontogenetic sequence of apertures, their centroids lie on a finite slice of a conical space curve (potentially, a conical logspiral), which is parameterized by the estimated apex and apical angle.

Testing that this space curve is actually a logspiral was done by fitting an exponential relationship for $r(\theta)$ (Eq.[1]) of centroids. Revolution angle, θ, is measured here in steps of half-revolution (i.e., 180°, or π radians). Similarly, an exponential relationship is sought for $z(\theta)$, in order to facilitate comparison with Schindel's and Larsson et al.'s longitudinal expansion rates, and, thus, assess spire allometry, k, and consistency with fitted conical envelopes. However, spire-height data in Collins et al. requires some special discussion.

Reanalysis of spire height in the Collins et al. dataset

In Collins et al.'s dataset, spire height is measured relative to a specimen-dependent arbitrary datum, taken to be the first (i.e., youngest) aperture in the ontogenetic sequence. Denoting this

measure of spire height by y, as in Collins et al. (2021a), the first sampled y-value is always $y = 0$. As Fig. 2 clearly demonstrates, number of sampled apertures varies markedly among specimens, even within the same species.

Collins et al. (2021b) correctly point out that, in such cases, there is a need for an intercept parameter that "accounts for the variation in starting point". However, the intercept parameter serves this function only when the response variable is y itself, not any (nonlinear) transform of y. For their "Exponential" (my logspiral), and "Power law" models, because they use linear formulas for model fitting, the response variable is log-transformed. In such cases, the intercept parameter loses its intended purpose of correcting variation in starting point. This is essentially "The Origin of Longitudinal Coordinates" problem that van Osselaer & Grosjean (2000) reviewed and discussed in detail, calling it "insidious" and a "pitfall that could lead to confusion with allometry".

Because it is exactly such exponential and power-law models that are of greatest interest, in light of Eq.[1], one must look for other ways to account for this starting-point variation. One method is to use the actual preserved apex of the shell, coinciding, more or less, with the top of the sampled coiling axes (Fig. 2). Although this procedure still contains errors "due to the uneven loss of starting whorls" (Collins et al. 2021b), it does, at least, reduce the variation in starting point.

A second, more rigorous, way is fitting nonlinear models to untransformed y-values. For the exponential case, that model takes the form

$$y = z_0(e^{(\gamma k)\theta} - 1) + \varepsilon, \qquad [3]$$

where ε is residual error, the fitted parameter z_0 represents a specimen-dependent starting value, and γk is the longitudinal expansion rate, per Eq.[1]. A three-parameter variant of Eq.[3] is $y = z_0 e^{(\gamma k)\theta} - c$, where c is a separate intercept parameter (equivalent to Eq.[15] of van Osselaer & Grosjean 2000). This modified formula has the added benefit of not forcing the fitted curve through $(0, 0)$ (i.e., through $y\big|_{\theta=0} = 0$), which may bias estimates of the exponential expansion rate, γk. In practice, though, both models produced very similar results.

Mixed-effect growth models

Testing for inter-clade differences, while accounting for individual variability in growth and allometry, was done with mixed-effect linear growth models (Grimm et al. 2017). The three main clades of the Collins et al. dataset are: *Maoricolpus roseus* (Turritellidae), *Tylospira*+*Perissodonta* (mostly *Tylospira coronata*), and the rest of the Struthiolariidae (mainly *Pelicaria vermis* and *Struthiolaria papulosa* specimens). (34, 25, and 88 specimens, respectively, out of total 162.) I estimated and tested for differences in allometric exponents and coiling parameters.

Data analytic procedures

Estimates of γ, k, $\cot\beta$, and $\tan\lambda$ from the datasets of Schindel and Noshita et al. are presented as is. Estimates derived from Larsson et al. (2020; Larsson & Butlin 2019) are additionally presented according to the two habitat types in that study, namely, either crab-predator- or wave-dominated. To simplify presentation, I divided specimens into two groups, according to their habitat score (negative [crab] or positive [wave]).

In the reanalysis of Collins et al., I additionally investigated growth and allometry by applying model selection (following Collins et al. 2021b, and adapting code from Collins et al. 2021a) to (*i*) conical envelopes, $y(r)$ or $r(y)$, from which $\cot\beta$ is estimated; (*ii*) radial expansion of centerline spirals, $r(\theta)$, from which γ is estimated; (*iii*) longitudinal expansion of centerline spirals, $y(\theta)$, from which γk (and consequently k) can be estimated; and (*iv*) aperture area, $A(\theta)$, $A(r)$ or $A(s)$, where s is empirically estimated arc length (i.e., cumulative length along the centerline spiral; see SI), from which k_w can be estimated. In addition, through the relationship between spire height and arc length, I estimated the lead angle, $\tan\lambda$ (details in SI).

All data analyses were done in `R` (version 4.3.3; R Core Team 2024). Models were compared by R^2_{adj} (or pseudo-R^2_{adj} for nonlinear models, using the `soilphysics` package; da Silva & de Lima 2015), and relative likelihood (from AIC_c-values, obtained with the `AICcmodavg` package; Mazerolle 2023). For fitting linear models, I used the `stats` base `R` package and the

lmodel2 package (Legendre 2024). Nonlinear models were fitted with nlsLM of the minpack.lm package (Elzhov et al. 2023). Mixed-effect growth models were applied with lmer of the lme4 package (Bates et al. 2015) and with the nlme package (Pinheiro et al. 2025), using procedures described in Grimm et al. (2017). I compared the three main clades in Collins et al. (2021a) through confidence intervals of coiling and allometry parameters.

As part of the reanalysis of Collins et al. (2021a), I also generated svg images (Fig. 2) from the original jpg files, for convenient visual inspection of fitted conical envelopes. The SI provides more details on data analytic procedures, as well as additional complementary results. I also wrote a WebGL program for generating images of shells (Fig. 1A,C-E; SI). All data, code and images are available in online repositories (see below and SI).

DRAFT

Results and Discussion

Goodness of fit of the conical logspiral model

Schindel (1990) previously suggested to replace Raup's coiling parameters with other, derived from loglinear regressions of shell width and spire height on revolution angle, θ. In terms of Eq.[1], these regression slopes are given by γ and γk, respectively. His parameters, therefore, are akin to coefficients of multivariate allometry (Klingenberg 1996), though he did not make that link. Schindel noticed that, unlike in Raup's morphospace, in the new parameter space the shells of sixty taxa show strong positive covariation. That is expected according to multivariate allometry, $\gamma k = \gamma$ means isometric growth. Fig. 3A presents Schindel's data, in terms of parameters γ and k of Eq.[1]. Scatter does not deviate much from isometry ($k = 1$), demonstrating that conical logspirals are reasonable first approximations for gastropod shells. Deviations are almost exclusively upwards, towards *doming* ($k > 1$; Vermeij 1980).

The larger dataset of Collins et al. (2021b) provided more detailed data on ontogenetic sequences of apertures, though not as taxonomically wide as Schindel (1990). Fig. 2 clearly demonstrates that conical envelopes fit the spatial configurations of centroids quite well. Major-axis type II regression (i.e., first principal axis of PCA) explained over 99% of total variance in spatial scatter of centroids, for all but 8 specimens (of these eight specimens, six had only four data points; see SI). These very good fits of conical envelopes are a strong indication that centerline spirals are indeed conical ($k = 1$ in Eq.[1]; $z \propto r$).

That is further corroborated by model selection. Of the four combinations of either a linear or a quadratic model, and either $y(r)$ or $r(y)$ regression, the best model was found to be linear regression of r on y (Table 1). Only 28 specimens (out of 162) showed statistically significant quadratic terms (at the 0.05 level), when applying $y(r)$ or $r(y)$ polynomial regressions. When applying Bonferroni correction (n =162), that number reduced to only two specimens (Fig. 2A,D).

Now that conical envelopes have been reasonably established, the next step is to test whether those space curves are slices of conical logspirals. Again applying model selection, the best-performing model for $r(\theta)$ was exponential, by linear regression of log-transformed

radii. Out of 162 specimens, only six exhibited marked deviation from logspiral, measured by R^2_{adj} lower than 0.9. These six specimens either belonged to the irregularly open-coiled *Tenagodus anguinus* or had only four data points. Only the *Tenagodus* specimens had R^2_{adj} lower than 0.84. The next best model (observed by removing the best) was the nonlinear exponential model (fitted with `nlsLM`). Similarly, for spire height, $y(\theta)$, the best-performing model was $\log(y + \text{offset}) \sim \theta$, where offset represents here specimen-specific correction, determined by the preserved apex of the shell, as described in Materials and Methods. The next best model was the nonlinear exponential of Eq.[3]. At this stage, I established conical envelopes, and $r(\theta)$ and $z(\theta)$ expanding exponentially. Namely, that the conical logspiral is the best-fitting model for centerline spirals.

I can now close the consistency loop, by providing estimates of k through ratios of estimated exponential growth rates of radii and spire height (γ and γk, respectively; Eq.[1]), which also facilitates comparison to Schindel's data (Fig. 3A). As Fig. 3B shows, estimates from linear regression models (i.e., the best preforming $\log(r) \sim \theta$ and $\log(y + \text{offset}) \sim \theta$) are similar to those obtained for Schindel's data (Fig. 3A). In particular, observe the high values for *Tenagodus* specimens, comparable to Schindel's *Truncatella valida* (syn. *guerinii*; upper-left of Fig. 3A), as both are roughly shaped as truncated cones, with a large initial radius at the top (Fig. 2K). It is, therefore, hardly surprising that corrections of spire-height, based on the actual preserved apices of shells, still result in a strong nonlinear $z(r)$ relationship, due to this relatively large initial radius, as discussed in Materials and Methods.

When k-estimates are derived from nonlinear exponential models (second-best model in Table 1; Eq.[3]), Fig. 3C clearly demonstrates that, once the need to correct spire height is circumvented by not transforming response variables, the conical logspiral ($k = 1$) is again supported. The high scatter in k-estimates is understandable, given the small sample sizes ($\leq$ 6) of more than half the specimens. Overall, comparing the three upper panels of Fig. 3 suggests that allometric exponents from Schindel (1990) are also confounded by this methodological problem of log-transformed spire height, as detailed in Materials and Methods.

Lastly, Larsson et al. (2020) have similarly found that longitudinal and radial expansion

rates are tightly linked and close to equal in their study of *Littorina saxatilis* (Fig. 3B,C). They reported consistently higher longitudinal rates, suggesting again that k is slightly over one. (95% of k-estimates from their data lie between 1.002 and 1.282, with mean 1.1258; comparable to values in Fig. 3C. In data from Garcia Castillo et al. 2024b, it is between 1.002 and 1.348, with mean 1.16.)

Aperture allometry, or "Behold, Plato's snail!"

The starting-point problem has plagued the study of shell morphology for many decades. van Osselaer & Grosjean (2000) provided a thoughtful discussion of its formulation and history (as well as of the sister problem of locating the coiling axis; Schindel 1990, Aldridge 1998, McGhee 2001, Larsson et al. 2020). They also analyzed data for several gastropod species, and found good fits to logarithmic spirals, at least piecewise. They additionally reanalyzed McGhee's (1980) data on the brachiopod *Lycophoria nucella*, which prompted a somewhat ungracious rebuttal by McGhee (2001), who did not conceal his dissatisfaction with a reanalysis of his data "after two decades", dubbing van Osselaer & Grosjean's "hypothetical logarithmic spiral" "a Platonic ideal", removed from "actual organisms" and "biological realities". These are typical straw man arguments (or plucked chicken arguments, keeping with the theme of ancient Greek philosophers) that themselves rely on implicit prejudices, such as an all-or-nothing approach. A far cry from Raup's practical and Gould's pluralistic attitudes (see end of Introduction).

Besides being ungracious, such an approach is also unscientific. A touch of "Platonic ideal" could have alerted Collins et al. (2021b) to incongruity in their Table 1, which showed good fit of "Exponential" models (i.e., logspiral) to data on aperture size, and columellar (umbilical) width (not considered here), but very poor performance for their spire height. An indication that there was something wrong with that analysis, as, ultimately, morphometric traits must combine to describe three-dimensional wholes in a consistent way.

Aperture shape clearly changes with aperture size in some of the shells in Fig. 2. Moreover, although the conical logspiral has been established for radial and longitudinal expansion of

centerline spirals (through fitted conical envelopes, exponential growth, and allometric exponents close to one; Fig. 3A,B,C, Table 1), I have not yet considered how the expansion and allometry of the apertures themselves relate to that of centerlines. Applying the same model selection procedure as before, I find (Table 1) that the best performing model is exponential $A(\theta)$, in accordance with the logspiral model. The next best model is power-law $A(r)$, which is expected, as elementary geometry dictates $A \propto r^2$ (though, if allometry occurs, the power-law exponent may be different than two; see next).

Comparing the allometric relationship $A(r)$ among clades, by applying mixed-effect growth models, I find that aperture size grows with slight positive allometry for *Maoricolpus* (high-spired Turritellidae), but with negative allometry for Sturthiolariidae — allometric exponent of aperture area is 2.11, 95%CI [2.073, 2.145], for *Maoricolpus*, 1.66 [1.59, 1.73] for *Tylospira* clade and 1.876 [1.845, 1.905] for the rest of Struthiolariidae. Within-clade standard deviation in allometric exponent among specimens is 0.0876 [0.0607, 0.1108], much lower than the inter-clade differences. The effect, in either direction (positive or negative allometry), however, is weak.

The larger deviation from an exponent of 2 for *Tylospira* may simply reflect stronger ontogenetic shape change of aperture in this clade, as well as wider and faster-expanding columella (clearly visible in Fig. 2F,G). But this pattern may also correspond to oversecretion of shell material, relative to soft-body growth, as suggested recently by Chirat et al. (2021). Accordingly, *Maoricolpus* (undersecretion; $k_w > 1$) are high-spired, and within Struthiolariidae the *Tylospira* clade is relatively low-spired (oversecretion; $k_w < 1$; Fig. 3D). Finally, I also note that these values for aperture allometry are in rough agreement with previously published estimates of aperture-area allometry, relative to body weight, for land snail species (Cameron 1981).

Covariation of coiling parameters, and adaptationist and mechanistic explanations

That Raup's three coiling parameters (W, D and T; Raup & Michelson 1965, Raup 1966), are "interdependent" is a piece of theoretical morphology folklore (Schindel 1990, Tursch 1997,

McGhee 1999). The often observed inverse relation between T and W has been taken as empirical demonstration of this nonindependence. From a dynamical system standpoint, however, Raup's whorl expansion parameter, W, solely determines the time evolution of the system (or θ-evolution in this case, as time is implicit). It remains to determine the initial conditions — initial size, r_0 (Eq.[1]), and initial shape, that are subsequently magnified by W. That is the role of T (or apical angle, β; Fig. 1B), and of D that divides r_0 between aperture and umbilicus (not considered explicitly in this work). From that viewpoint, Raup's W-D-T parameters are independent of each other. As I discussed above, considerations of multivariate allometry, in fact, make Schindel's (1990) coiling parameters interdependent.

Generally speaking, empirically observed covariation in coiling parameters, and uneven distributions of species within morphospaces, often receive adaptationist interpretations, such as mechanical strength, postural stability or economical shell construction (Raup 1966, Noshita et al. 2012, Okabe & Yoshimura 2017, Páll-Gergely et al. 2024). However, for small γ, typical of most gastropods, this covariation may also be explained by seemingly arbitrary conditions on lead angle. Specifically, Raup's (1966) condition for tight coiling, or whorl overlap, given circular apertures, $\tan\beta > \sinh(\pi\gamma)$, is practically indistinguishable from the condition $\lambda < \operatorname{atan}(1/\pi)$ (0.318 or 17.66°; Fig. 3D; SI). Similar conditions can be formulated for non-circular apertures (Fig. 3D; Eq.[S15] in SI).

A geometric constraint on lead angle, combined with variation in growth rate (shell expansion), can produce (given Eq.[2]) the empirically observed direct relation between $\tan\beta$ and γ (equivalent to the familiar inverse relationship between Raup's T and W; Raup 1966, SI). Fig. 3E shows estimates of lead angle for the different datasets that are reanalyzed in this study. For shells from Collins et al., different clades cluster around typical values of λ that seem independent of variation in γ. A mixed-effect linear growth model (SI) estimated $\tan\lambda$ at 0.421 [0.417, 0.425] for *Maoricolpus*, 0.281 [0.267, 0.294] for the *Tylospira* clade, and 0.325 [0.322, 0.327] for rest of the Struthiolariidae. Variation in apical angle (β; Fig. 3D) follows as a passive consequence of growth (variation in γ) and geometry (lead angle, λ) of the expanding centerline spiral (by means of Eq.[2]), providing a way for "moving the β

parameter down to the mantle edge" (Løvtrup & Løvtrup 1988). It is important to note that these estimates of lead angle are not affected by the longitudinal starting-point problem, as they depend only on differences (or rate of change) in the z-coordinate.

The three-way relation between lead angle, apical angle and expansion rate, prescribed in Eq.[2], also helps to explain the association of high-spired species with large numbers of whorls (Cain 1980) and Gould's so-called "jigsaw constraint", originally observed in his study of *Cerion* (Gould 1989, Béguinot 2021). For a fixed lead angle, $\tan\lambda \approx const$, Eq.[2] translates to a linear relationship between apical angle, $\tan\beta$, and expansion rate, γ. As a result, higher spired shells (smaller β) expand less per full revolution, and require more whorls to reach a given size. Lastly, adopting γ and λ as the natural axes of coiling behavior (Fig. 3E) is also strongly supported by experiments and observations on within-species developmental plasticity (e.g., scalariforms or "corkscrew"s), and effects of variation in soft-body growth on shell morphology (Vermeij 1980, 1993, Kemp & Bertness 1984, Arendt 1997, 2015, Checa et al. 1998, van der Sman et al. 2009, Clewing et al. 2015, Larsson et al. 2020).

Growth map models (Fig. 1E; SI; Rice 1998, Ubukata 2003, Hammer & Bucher 2005, Urdy et al. 2010) and the differential geometry tradition in theoretical morphology (Okamoto 1988, Noshita 2014, Goriely 2017, Chirat et al. 2021, Ohta et al. 2025) similarly attempt to explain global shell shape by explicitly modeling differential growth rates and directions around a shell's aperture. The latter approach describes shell coiling in terms of *curvature* and *torsion* (in the differential geometry sense) of centerline curves (Okamoto 1988, Chirat et al. 2021, Ohta et al. 2025). The ratio of torsion to curvature is an alternative way to define $\tan\lambda$.

The original formulation of logspiral shells was in terms of fixed spiral angles (hence, the term equiangular spiral, used interchangeably with logarithmic spiral; Thompson [1942] 1992), defined as the angle between the conical apex (or pole of the spiral), a point on the (helico)spiral, and the tangent to the spiral at that point, all lying on the surface of the conical envelope (Fig. 1B). Denoting spiral angle by α, one can rewrite Eq.[2] as covariation of expansion rate, apical angle and spiral angle, instead of lead angle, i.e., $\cot\alpha\sin\beta = \gamma$ (Eq.[S1]; Moseley 1842, Thompson [1942] 1992, Raup & Graus 1972, Løvtrup & von Sydow

1974, Illert 1983). The observed covariation of coiling parameters, therefore, can also be interpreted in terms of a constant spiral angle, $\cot\alpha = const$ (see SI and Fig. S1 for more details). However, I stick in this work with the lead angle, λ, because it is more straightforward to estimate from sectioned specimens and photographs, because in this study all shells are far from planispiral, because Raup's model is in terms of T ($= \cot\beta$; or $\tan\beta = 1/T$; rather than $\sin\beta$), and because lead angle has an easy interpretation as torsion-curvature ratio, thus, providing a link between *moving-frame* formulations (Okamoto 1988, Ackerly 1989; growth maps and differential geometry) and fixed coordinate system models (Fig. 1A,B).

Taking the multispiral standpoint, helicospirals on the shell (Fig. 1D), designated by position on the aperture's perimeter, φ (Fig. 1F), differ in torsion-curvature ratios, or $\tan\lambda$. For allometrically growing shells, torsion-curvature ratios also vary ontogenetically within each spiral. In terms of developmental plasticity, variation in curvature-torsion that anyhow occurs among helicospiral paths, also in the isometric case, is manifested within each such path in the allometric case. A shell's aperture, therefore, dictates a gradient in lead angle (Fig. 1D,F,G),

$$\frac{\mathrm{d}\lambda}{\mathrm{d}\varphi} \approx \frac{\gamma}{\sin^2\beta + \gamma^2\cos^2\beta}\left(-\frac{\mathrm{d}\beta}{\mathrm{d}\varphi}\right) \qquad [4]$$

(Eq.[2], SI). This gradient determines how neighboring helicospiral paths on the shell's surface diverge in lead angle. Typically, as one moves abapically along the perimeter of the aperture, spirals are initially roughly parallel ($\mathrm{d}\beta/\mathrm{d}\varphi$ vanishes in Eq.[4]; Fig. 1D). As the aperture begins to close, both factors in Eq.[4] become larger, causing increasing divergence of spiral paths in both abapical and adaxial direction (Fig. 1D,F) — a geometric consequence of logspiral coiling. Rates and directions of cellular growth and division that are correlated with this gradient (Johnson et al. 2019, Ohta et al. 2025) are, therefore, a null expectation, for both isometric and allometric shell growth. In developmental plasticity parlance, whether the cellular processes are "leaders" or "followers" (West-Eberhard 2003) remains, however, to be determined. Moreover, previously formulated challenges to fine control of global shell form in gastropods by apertural growth rates still remain (Hutchinson 1990).

Conclusion

In this work, I brought together, under a revised theoretical-morphological model, diverse observations on (piecewise) regularity in coiling (in gastropods and other shelly forms), on patterns of covariation in morphometric traits and coiling parameters, on shell growth and morphogenesis at the cellular level, and on developmental plasticity in gastropods. This model integrates several approaches to theoretical morphology of coiled shells, provides a bridge between empirical studies and theoretical shell models, as advocated by Gould (1984) and Liew & Schilthuizen (2016), and is backed by extensive statistical analyses that combined basic geometry, multimodel inference, mixed-effect models, and several datasets, to obtain general insights into variation in coiling behavior. On the way, I also presented a solution to the pesky longstanding methodological problem of longitudinal origin of measurement, and its confusion with allometry (van Osselaer & Grosjean 2000).

In the manner of D'Arcy Thompson (Thompson [1942] 1992), spiral geometry, particularly logspiral, dictates certain "laws" for coiled shells. Centerline spirals of gastropods follow quite well conical logarithmic spirals. Allometry, while common, remains relatively weak, manifesting mostly in the aperture's expansion and shape change, relative to radial centerline expansion. Theoretical arguments and empirical patterns (Fig. 3D,E) suggest the lead angle (λ) as a more biologically sensible parameter for understating coiling behavior, compared to apical angle (β) or Raup's translation parameter (T). The three-way relationship between expansion rate, apical angle and lead angle, $\tan\beta\tan\lambda \approx \gamma$ (Eq.[2]), helps to explain empirically observed intra- and interspecific associations between narrow (high) spires and low expansion rates or high numbers of whorls (Fig. 3D; Cain 1980, Gould 1989). It also helps to explain, through the inverse relationship between apical and lead angles, for a given expansion rate, patterns of divergence in rates and directions of cellular growth around a shell aperture (or mantle; Eq.[4]; Fig. 1D,F,G; Johnson et al. 2019).

In past studies (Schindel 1990, Collins et al. 2021b), allometry of spire height was confounded with the methodological problem of starting-point variation, or unknown longitudinal origin (van Osselaer & Grosjean 2000). When this effect is correctly accounted

for, through fitting nonlinear models to untransformed response variables, I observe allometric exponents that are clustered close to one (i.e, isometry), consistent with the conical envelopes of centerline spirals (Fig. 2). As others before (van Osselaer & Grosjean 2000), I argue that significant allometry is confined to the protoconch-teleconch transition and, therefore, the geometric apex of conical logspirals is usually located outside the actual shell. This claim should be further scrutinized for terrestrial gastropods, known to commonly exhibit doming (Gould 1969, 1984, Goodfriend 1983, Vermeij 1993).

More broadly, such geometric relationships are useful in defining natural axes of variation for data analyses and in integrating data from several sources, obtained by different methodologies (Fig. 3). In the spirit of Gould (1984), of combining "deductive" and "inductive" approaches to morphology, I demonstrated the dangers in relying on only a single technique, powerful as it may be, and in indiscriminately applying generic formulas and workflows. Even in an age of ever more sophisticated statistical machinery, common sense practices, of applying several methods of analysis, and consistency checks, should not be forgotten (e.g., geometric, visual, mathematical modeling, applying different statistical methods, and considering how individual traits combine to form consistent wholes).

Adaptationist approaches should similarly acknowledge alternative, often indistinguishable, explanations that emerge from such "laws of form" (Fig. 3D,E). A final application is in addressing the perennial topic, in paleobiology and evolutionary biology, of interpreting spatiotemporal patterns of morphological diversity, in light of interchangeability of genetic and environmental influences (West-Eberhard 2003) and widely observed developmental and intraspecific plasticity in growth and form.

Acknowledgements

I thank Inon Scharf, Ofer Ovadia, Rodrigo B. Salvador, and two anonymous reviewers for their time, patience and valuable comments on previous drafts of this paper. I thank Cristian Seres for aid with verification of digitized datasets. Images in Fig. 1F,G from Raup (1961) and Johnson et al. (2019), reproduced here under fair use and conditions of the PNAS license. The original illustrations of *Ecphora* (Fig. 1F) are by John S. Spurbeck.

DATA AND SOFTWARE AVAILABILITY. All data, code and images (except original images for Fig. 1F,G) are available at https://doi.org/10.5281/zenodo.15723486. Web app for theoretical morphology of coiled shells (Fig. 1A,C-E) is available at https://doi.org/10.5281/zenodo.15518552.

DRAFT

References

Ackerly, S.C. 1989. Kinematics of accretionary shell growth, with examples from barchiopods and molluscs. *Paleobiology* **15**: 147–164.

Aldridge, A. 1998. Brachiopod outline and the importance of the logarithmic spiral. *Paleobiology* **24**: 215–226.

Araki, A. & Noshita, K. 2023. Theoretical morphological analysis of differential morphospace occupation patterns for terrestrial and aquatic gastropods. *Evolution* **77**: 1864–1873. https://doi.org/10.1093/evolut/qpad110.

Arendt, J. 2015. Why get big in the cold? size–fecundity relationships explain the temperature-size rule in a pulmonate snail (*Physa*). *J. Evol. Biol.* **28**: 169–178.

Arendt, J.D. 1997. Adaptive intrinsic growth rates: an integration across taxa. *Q. Rev. Biol.* **72**: 149–177.

Bates, D., Mächler, M., Bolker, B. & Walker, S. 2015. Fitting linear mixed-effects models using lme4. *Journal of Statistical Software* **67**: 1–48. 10.18637/jss.v067.i01.

Bayer, U. 1978. Morphogenetic programs, instabilities, and evolution — a theoretical study. *Neues Jahrb. Geol. Paläont. Abh.* **156**: 226–261.

Béguinot, J. 2021. Adult shell-size regulation in conispirally-coiled shells: evidence for a widespread negative covariance between whorls growth-rate and the final number of whorls in land snails. *Annual Research & Review in Biology* **36**: 95–106. https://doi.org/10.9734/arrb/2021/v36i1030439.

Bookstein, F.L. 1978. *The measurement of biological shape and shape change*. Lecture notes in biomathematics. Springer-Verlag, Berlin.

Cain, A.J. 1980. Whorl number, shape, and size of shell in some pulmonate faunas. *J. Conchol.* **30**: 209–221.

Cameron, R.A.D. 1981. Functional aspects of shell geometry in some british land snails. *Biol. J. Linn. Soc.* **16**: 157–167. https://doi.org/10.1111/j.1095-8312.1981.tb01648.x.

Checa, A.G., Jimenez-Jimenez, A.P. & Rivas, P. 1998. Regulation of spiral coiling in the terrestrial gastropod *Sphincterochila*: an experimental test of the road holding model. *J. Morphol.* **235**: 249–257.

Chirat, R., Goriely, A. & Moulton, D.E. 2021. The physical basis of mollusk shell chiral coiling. *Proc. Natl. Acad. Sci. U.S.A.* **118**. https://doi.org/10.1073/pnas.2109210118.

Clewing, C., Riedel, F., Wilke, T. & Albrecht, C. 2015. Ecophenotypic plasticity leads to extraordinary gastropod shells found on the ”roof of the world”. *Ecol. Evol.* **5**: 2966–2979. https://europepmc.org/articles/PMC4541999.

Collins, K.S., Klapaukh, R., Crampton, J.S., Gazley, M.F., Schipper, C., Maksimenko, A. & Hines, B.R. 2021a. Data associated with: Going round the twist — an empirical analysis of shell coiling in helicospiral gastropods. Dryad Dataset. https://doi.org/10.5281/zenodo.12159344.

Collins, K.S., Klapaukh, R., Crampton, J.S., Gazley, M.F., Schipper, C., Maksimenko, A. & Hines, B.R. 2021b. Going round the twist—an empirical analysis of shell coiling in helicospiral gastropods. *Paleobiology* **47**: 648–665. https://doi.org/10.1017/pab.2021.8.

Cortie, M. 1989. Models for mollusc shell shape. *South African Journal of Science* **85**: 454–460.

da Silva, A.R. & de Lima, R.P. 2015. soilphysics: an R package to determine soil preconsolidation pressure. *Computers and Geosciences* **84**: 54–60.

Edie, S.M., Collins, K.S. & Jablonski, D. 2024. Testing for allocation strategies and evolutionary tradeoffs in the bivalve shell. *J. Molluscan Stud.* **90**: eyae047. https://doi.org/10.1093/mollus/eyae047.

Elzhov, T.V., Mullen, K.M., Spiess, A.N. & Bolker, B. 2023. *minpack.lm: R Interface to the Levenberg-Marquardt Nonlinear Least-Squares Algorithm Found in MINPACK, Plus Support for Bounds*. https://CRAN.R-project.org/package=minpack.lm. R

package version 1.2-4.

Fowler, D.R., Meinhardt, H. & Prusinkiewicz, P. 1992. Modeling seashells. In: *Proceedings of the 19th annual conference on Computer graphics and interactive techniques*, pp. 379–387. 10.1145/133994.134096.

Garcia Castillo, D., Barton, N., Faria, R., Larsson, J., Stankowski, S., Butlin, R., Johannesson, K. & Westram, A.M. 2024a. Data and code for: Predicting rapid adaptation in time from adaptation in space: a 30-year field experiment in marine snails. Zenodo Dataset. https://doi.org/10.5281/zenodo.12159344.

Garcia Castillo, D., Barton, N., Faria, R., Larsson, J., Stankowski, S., Butlin, R., Johannesson, K. & Westram, A.M. 2024b. Predicting rapid adaptation in time from adaptation in space: A 30-year field experiment in marine snails. *Sci. Adv.* **10**: eadp2102. https://dx.doi.org/10.1126/sciadv.adp2102.

Goodfriend, G. 1983. Some new methods for morphometric analysis of gastropod shells. *Malacological. Review.* **16**: 79–86.

Goriely, A. 2017. *The Mathematics and Mechanics of Biological Growth*. Springer. https://doi.org/10.1007/978-0-387-87710-5.

Gould, S.J. 1969. An evolutionary microcosm: pleistocene and recent history of the land snail *P. poecilozonites* in bermuda. *Bulletin of the Museum of Comparative Zoology* **138**: 407–532.

Gould, S.J. 1984. Morphological channeling by structural constraint: convergence in styles of dwarfing and gigantism in *Cerion*, with a description of two new fossil species and a report on the discovery of the largest *Cerion*. *Paleobiology* **10**: 172–194.

Gould, S.J. 1989. A developmental constraint in *Cerion*, with comments on the definition and interpretation of constraint in evolution. *Evolution* **43**: 516–539.

Grimm, K.J., Ram, N. & Eastabrook, R. 2017. *Growth Modeling: Structural Equation and Multilevel Modeling Approaches*. Guilford Press, New York.

Hammer, Ø. 2016. *Perfect Shape: Spiral Stories*. Springer.

Hammer, Ø. & Bucher, H. 2005. Models for the morphogenesis of the molluscan shell. *Lethaia*. **38**: 111–122.

Hutchinson, J.M.C. 1990. Control of gastropod shell form via aperture growth rates. *J. Morphol.* **206**: 259–264.

Huxley, J.S. [1932] 1993. *Problems of relative growth (with a new introduction by Frederick B. Churchill and an essay by Richard E. Strauss)*. Johns Hopkins University Press, Baltimore.

Illert, C. 1983. The mathematics of gnomonic seashells. *Math. Biosci.* **63**: 21–56.

Johnson, A.B., Fogel, N.S. & Lambert, J.D. 2019. Growth and morphogenesis of the gastropod shell. *Proc. Natl. Acad. Sci. U.S.A.* **116**: 6878 – 6883. https://doi.org/10.1073/pnas.1816089116.

Kemp, P. & Bertness, M.D. 1984. Snail shape and growth rates: evidence for plastic shell allometry in *Littorina littorea*. *Proc. Natl. Acad. Sci. U.S.A.* **81**: 811–813. https://doi.org/10.1073/pnas.81.3.811.

Klingenberg, C.P. 1996. Multivariate allometry. In: *Advances in Morphometrics* (L.F. Marcus, M. Corti, A. Loy, G.J.P. Naylor & D.E. Slice, eds), vol. 284 of *NATO Advanced Science Institutes Series*, pp. 23–49. Plenum Press, New York.

Larsson, J. & Butlin, R. 2019. Shape variation in *Littorina saxatilis* ecotype contact zones. Dataset. https://dx.doi.org/10.15131/shef.data.9944462.v1.

Larsson, J., Westram, A.M., Bengmark, S., Lundh, T., Butlin, R.K. & Butlin, R.K. 2020. A developmentally descriptive method for quantifying shape in gastropod shells. *J. R. Soc. Interface* **17**. http://dx.doi.org/10.1098/rsif.2019.0721.

Legendre, P. 2024. *lmodel2: Model II Regression*. https://CRAN.R-project.org/package=lmodel2. R package version 1.7-4.

Liew, T.S., M., K.A.C., M., S. & S., U. 2014. On growth and form of irregular coiled-shell of a terrestrial snail: *Plectostoma concinnum* (Fulton, 1901) (Mollusca: Caenogastropoda: Diplommatinidae). *PeerJ* **2**: e383. https://doi.org/10.7717/peerj.383.

Liew, T.S. & Schilthuizen, M. 2016. A method for quantifying, visualising, and analysing

gastropod shell form. *PLOS ONE* **11**: 1–24. https://doi.org/10.1371/journal.pone.0157069.

Løvtrup, S. & Løvtrup, M. 1988. The morphogenesis of molluscan shells: a mathematical account using biological parameters. *J. Morphol.* **197**: 53–62.

Løvtrup, S. & von Sydow, B. 1974. D'arcy Thompson's theorem and the shape of the molluscan shell. *Bull. Math. Biol.* **36**: 567–575.

Mazerolle, M.J. 2023. *AICcmodavg: Model selection and multimodel inference based on (Q)AIC(c)*. https://cran.r-project.org/package=AICcmodavg. R package version 2.3.3.

McGhee, G.R. 1980. Shell form in the biconvex articulate brachiopoda: a geometric analysis. *Paleobiology* **6**: 57–76.

McGhee, G.R. 1999. *Theoretical Morphology : The Concept and Its Applications*. Perspectives in Earth History and Paleobiology. Columbia University Press, New York.

McGhee, G.R. 2001. The question of spiral axes and brachiopod shell growth: a comparison of morphometric techniques. *Paleobiology* **27**: 716–723. https://doi.org/10.1666/0094-8373(2001)027<0716:TQOSAA>2.0.CO;2.

Moseley, H. 1838. On the geometrical forms of turbinated and discoid shells. *Philosophical Transactions of the Royal Society of London* **1838**: 351–370.

Moseley, H. 1842. On conchyliometry. *Lond. Edinb. Dubl. Phil. Mag.* **21**: 300–305.

Noshita, K. 2014. Quantification and geometric analysis of coiling patterns in gastropod shells based on 3d and 2d image data. *J. Theor. Biol.* **363**: 93–104.

Noshita, K., Asami, T. & Ubukata, T. 2011. Data from: Functional constraints on coiling geometry and aperture inclination in gastropods. Dryad Dataset. https://doi.org/10.5061/dryad.6mk023c0.

Noshita, K., Asami, T. & Ubukata, T. 2012. Functional constraints on coiling geometry and aperture inclination in gastropods. *Paleobiology* **38**: 322–334. 10.1666/10060.1.

Ohta, S., Noshita, K., Kimoto, K., Ishikawa, A., Sato, H., Shimizu, K. & Endo, K. 2025. Wnt

activation causes shell malformation in lymnaeoidean gastropods. *J. Molluscan Stud.* **91**: eyaf001. https://doi.org/10.1093/mollus/eyaf001.

Okabe, T. & Yoshimura, J. 2017. Optimal designs of mollusk shells from bivalves to snails. *Scientific Reports* **7**: 42445. https://doi.org/10.1038/srep42445.

Okamoto, T. 1988. Analysis of heteromorph ammonoids by differential geometry. *Paleobiology* **31**: 35–52.

Páll-Gergely, B., Sipos, A.Á., Harzhauser, M., Örstan, A., Winkler, V. & Neubauer, T.A. 2024. Many roads to success: alternative routes to building an economic shell in land snails. *Evolution* **78**: 778–786. https://doi.org/10.1093/evolut/qpae018.

Pinheiro, J., Bates, D. & R Core Team 2025. *nlme: Linear and Nonlinear Mixed Effects Models*. https://CRAN.R-project.org/package=nlme. R package version 3.1-168.

Prusinkiewicz, P. & Fowler, D.R. 2009. Chapter 10: Shell models in three dimensions. In: Meinhardt H, *The Algorithmic Beauty of Sea Shells*, 4th edn, pp. 166–185. Springer, Berlin, Heidelberg. https://doi.org/10.1007/978-3-540-92142-4_10.

R Core Team 2024. *R: A Language and Environment for Statistical Computing*. R Foundation for Statistical Computing, Vienna, Austria. https://www.R-project.org/.

Raup, D.M. 1961. The geometry of coiling in gastropods. *Proc. Natl. Acad. Sci. U.S.A.* **47**: 602–609. https://doi.org/10.1073/pnas.47.4.602.

Raup, D.M. 1966. Geometric analysis of shell coiling: general problems. *J. Paleontol.* **40**: 1178–1190.

Raup, D.M. & Graus, R.R. 1972. General equations for volume and surface area of a logarithmically coiled shell. *Mathematical Geology* **4**: 307–316.

Raup, D.M. & Michelson, A. 1965. Theoretical morphology of the coiled shell. *Science* **147**: 1294–1295.

Rice, S.H. 1998. The bio-geometry of mollusc shells. *Paleobiology* **24**: 133–149.

Savazzi, E. 1990. Biological aspects of theoretical shell morphology. *Lethaia.* **23**: 195–212.

Savazzi, E. 1996. Adaptaions of vermetid and siliquarid gastropods. *Palaeontology* **39**: 157–177.

Schindel, D.E. 1990. Unoccupied morphospace and the coiled geometry of gastropods: architectural constraint or geometric covariation? In: *Causes of Evolution: a paleontological perspective* (R. Ross & W. Allmon, eds), pp. 270–304. University of Chicago Press, Chicago.

Seilacher, A. 1973. Fabricational noise in adaptive morphology. *Syst. Biol.* **22**: 451–465. https://doi.org/10.2307/2412952.

Stone, J.R. 1995. Cerioshell: a computer program designed to simulate variation in shell form. *Paleobiology* **21**: 509–519.

Stone, J.R. 1996. The evolution of ideas: a phylogeny of shell models. *Am. Nat.* **148**: 904–929.

Swan, A.R.H. 2015. Heterochrony in helicoid spiral cones: a computer model for demonstrating heterochronic evolution. *Palaeontologia Electronica* **18**: 1–11. 10.26879/510.

Thompson, D.W. [1942] 1992. *On Growth and Form: The Complete Revised Edition*. Dover, New York.

Tursch, B. 1997. Spiral growth: The 'Museum of all shells' revisited. *J. Molluscan Stud.* **63**: 547–554. https://doi.org/10.1093/mollus/63.4.547.

Ubukata, T. 2003. Pattern of growth rate around aperture and shell form in bivalvia: a theoretical morphological study. *Paleobiology* **29**: 480–491.

Urdy, S. 2015. Theoretical modelling of the molluscan shell: What has been learned from the comparison among molluscan taxa? In: *Ammonoid Paleobiology: From anatomy to ecology* (C. Klug, D. Korn, K. De Baets, I. Kruta & R.H. Mapes, eds), pp. 207–251. Springer Netherlands, Dordrecht. https://doi.org/10.1007/978-94-017-9630-9_6.

Urdy, S., Goudemand, N., Bucher, H. & Chirat, R. 2010. Allometries and the morphogenesis of the molluscan shell: a quantitative and theoretical model. *J. Exp. Zool.* **314B**: 280–302. 10.1002/jez.b.21337.

van der Sman, J., Phillips, N.E. & Pfister, C.A. 2009. Relative effects of maternal and juvenile food availability for a marine snail. *Ecology* **90**: 3119–3125.

van Osselaer, C. & Grosjean, P. 2000. Suture and location of the coiling axis in gastropod shells. *Paleobiology* **26**: 238–257. https://doi.org/10.1666/0094-8373(2000)026<0238:SALOTC>2.0.CO;2.

Vermeij, G.J. 1980. Gastropod shell growth rate, allometry, and adult size. In: *Skeletal Growth of Aquatic Organisms* (D. Rhoads & R. Lutz, eds), pp. 379–393. Plenum Press, New York.

Vermeij, G.J. 1993. *A Natural History of Shells*. Princeton University Press, Princeton, Oxford.

West-Eberhard, M.J. 2003. *Developmental plasticity and evolution*. Oxford University Press, New York.

DRAFT

Table 1: Model selection for conical envelopes, centerline spire height, centerline spiral radii, and aperture area. Formulas of models are presented in a form that is loosely based on R's formula format. Mean R^2_{adj} are given, as well as the mean (per-specimen) relative likelihood of each model, and similarly obtained mean relative likelihoods after removing the best model. The model-dependent symbols b, c, c_0 and c_1 represent general fitted parameters, not otherwise defined in the main text. Linear models with log-transformed (response or predictor) variables implicitly include a small correction value of 0.0001, to avoid $\log(0)$ (as in Collins et al. 2021b). (More details on model selection procedures in SI.)

Model	Mean R^2	Mean relative likelihood	Mean relative likelihood (best removed)
Conical envelope: $y(r)$ or $r(y)$			
Linear $y(r)$, $y \sim r$	0.96178	0.00062	–
Linear $r(y)$, $r \sim y$	0.96178	0.75398	–
Quadratic $y(r)$, $y \sim \texttt{poly}(r, 2)$	0.96472	0.01266	–
Quadratic $r(y)$, $r \sim \texttt{poly}(y, 2)$	0.96803	0.32830	–
Spire height: $y(\theta)$			
Log, $y \sim \log\theta$	0.26883	<0.00001	<0.00001
Exponential, $\log(y) \sim \theta$	0.46551	<0.00001	<0.00001
Power-law w/ offset, $\log(y + \text{offset}) \sim \log\theta$	0.47520	0.00001	0.01201
`nls` Power-law w/ offset, $(y + \text{offset}) \sim (c_1\theta + c_0)^b$	0.95570	0.09104	0.16710
Linear, $y \sim \theta$	0.96074	0.00002	0.00004
Exponential w/ offset, $\log(y + \text{offset}) \sim \theta$	0.98733	0.81401	–
`nls` 3-parameter Exponential, $y \sim z_0 e^{(\gamma k)\theta} - c$	0.98995	0.09179	0.14979
`nls` Exponential w/ offset, $(y + \text{offset}) \sim z_0 e^{(\gamma k)\theta}$	0.99120	<0.00001	0.03367
Quadratic, $y \sim \texttt{poly}(\theta, 2)$	0.99175	0.09491	0.11053
`nls` Exponential, $y \sim z_0(e^{(\gamma k)\theta} - 1)$	0.99417	0.07097	0.49509
Power-law, $\log(y) \sim \log\theta$	0.99619	0.01445	0.44627
Spiral radius: $r(\theta)$			
Log, $r \sim \log\theta$	0.27773	0.00002	0.00006
Power-law, $\log(r) \sim \log\theta$	0.44605	0.00542	0.09722
Linear, $r \sim \theta$	0.94537	0.00547	0.17107
`nls` Power-law, $r \sim (c_1\theta + c_0)^b$	0.96906	0.10776	0.26471
`nls` Exponential, $r \sim r_0 e^{\gamma\theta}$	0.97041	0.00440	0.66115
Exponential, $\log(r) \sim \theta$	0.97054	0.84584	–
Quadratic, $r \sim \texttt{poly}(\theta, 2)$	0.97345	0.14283	0.25191
Aperture size: $A(\theta)$, $A(s)$, or $A(r)$			
Power-law, $\log(A) \sim \log\theta$	0.50233	0.00225	0.00226
`nls` Power-law, $A \sim (c_1\theta + c_0)^b$	0.77168	0.00344	0.00344
Log, $A \sim \log\theta$	0.84434	<0.00001	<0.00001
Linear, $A \sim \theta$	0.88939	<0.00001	<0.00001
Exponential, radius, $\log(A) \sim r$	0.90444	0.00675	0.02528
Exponential, arc length, $\log(A) \sim s$	0.92734	0.08308	0.21283
`nls` Exponential, radius, $A \sim A_0 e^{cr}$	0.93772	<0.00001	<0.00001
Power-law, arc length, $\log(A) \sim \log(s)$	0.93990	0.22106	0.28947

Linear, radius, $A \sim r$	0.94093	<0.00001	<0.00001
`nls` Exponential, arc length, $A \sim A_0 e^{cs}$	0.94489	<0.00001	<0.00001
`nls` Power-law, radius, $A \sim (c_1 r + c_0)^b$	0.95862	0.01223	0.01223
Linear, arc length, $A \sim s$	0.95985	<0.00001	<0.00001
Quadratic, arc length, $A \sim \texttt{poly}(s, 2)$	0.95985	<0.00001	<0.00001
Quadratic, radius, $A \sim \texttt{poly}(r, 2)$	0.96105	0.02046	0.02046
Power-law, radius, $\log(A) \sim \log(r)$	0.96774	0.36734	0.55091
Exponential, $\log(A) \sim \theta$	0.97222	0.42050	–
Quadratic, $A \sim \texttt{poly}(\theta, 2)$	0.97232	0.00458	0.00458
`nls` Exponential, $A \sim A_0 e^{(2\gamma k_w)\theta}$	0.98053	<0.00001	<0.00001
`nls` Power-law, arc length, $A \sim (c_1 s + c_0)^b$	0.98508	0.10351	0.10352

DRAFT

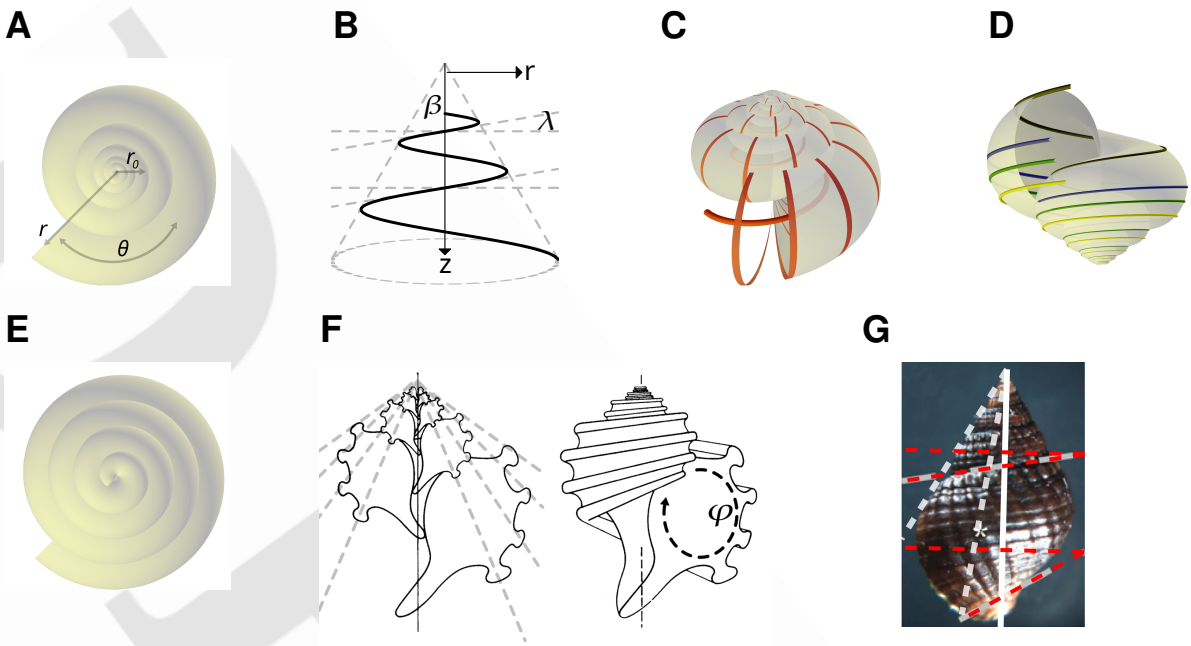

Figure 1 : Theoretical morphology in a snailshell. (***A***) Logspiral shell in apical view. Radius, r, revolution angle, θ, and initial size, $r_0 = r(\theta = 0)$, are illustrated. (***B***) Conical logspiral in lateral view. (Half-)Apical angle, β, and lead angle, λ, are defined. (***C***) Generating curve approach to shell modeling. Shell surface defined by a closed figure (here a circle) that sweeps along a centerline logspiral. (***D***) Multispiral approach to shell modeling, where shell surface is defined by many spiral paths, differing in lead angle. Uppermost (black) spiral most inclined, as it lies closest to the coiling axis. (***E***) Growth map models show that a combination of linear growth (constant growth rate) and a fixed centerline lead angle produces domed shells ($k \approx 2$). But such shells are unnaturally characterized by Archimedean, rather than logarithmic, spirals (SI). (***F***) Helicospirals around a shell can be parametrized by position on the perimeter of the aperture, φ (e.g., azimuth angle, if applicable, as in Larsson et al. (2020); or a general parameterization, such as φ running from 0 to 1 along the perimeter, or $\varphi \in [0, L]$ (Goriely 2017), where L is the length of the perimeter of the generating curve), demonstrated here by adopting the pretty illustrations of *Ecphora* by John S. Spurbeck (Raup 1961). Apical angle (left) and lead (right) vary among spiral paths. γ estimated at 0.152 (slightly higher than Raup's reported value). Measured angles are β = 54.45°, 44.75°, 34.71°, 23.02° and λ = 6.65°, 9.17°, 15.16°, 21.64°. Close to theoretical λ-values (Eq.[2]) of 6.22°, 8.77°, 12.56°, 20.47°, respectively. (***G***) A similar demonstration using the *Tritia* shell from Johnson et al. (2019). γ = 0.0825°. Upper (suture) spiral: β = 30.61°, λ = 9.7°. Lower (abapical) spiral: β = 9.1°, λ = 30.14°. Again, λ-values close to theoretical values of 8° and 29.51°, respectively, as the conical logspiral model predicts.

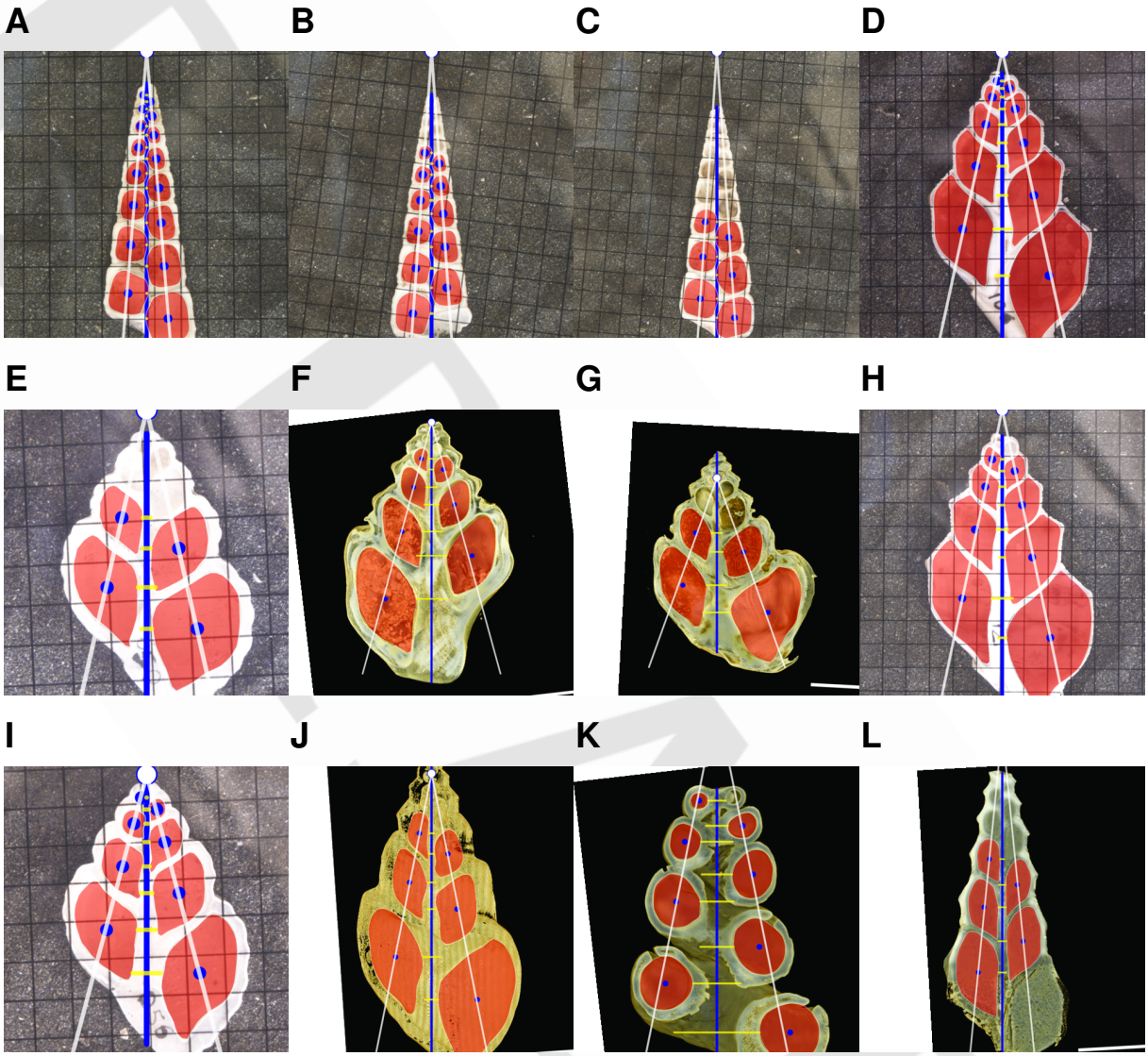

Figure 2 : Some examples of sectioned shells from the dataset of Collins et al. (2021a). As part of the reanalysis done in this paper, I generated `svg` images, with highlighted apertures (shaded red), and illustrated aperture centroids (blue dots), coiling axis (blue line), measured columella (umbilicus) widths (yellow), estimated apex of conical envelope (white dot) and estimated apical angle (white lines). Compared to the originals, the generated `svg` images have been zoomed in on the specimens and rotated, such that the measured coiling axis (blue line) is vertical. (***A,B,C***) Specimens of *Maoricolpus roseus* (Turritellidae): specimen IDs `071`, `082` and `073`, respectively. (***D,H***) Specimens of *Struthiolaria papulosa* (Struthiolariidae): specimen IDs `106` and `121`, respectively. (***E,I***) Specimens of *Pelicaria vermis* (Struthiolariidae): specimen IDs `050` and `056`, respectively. (***F,G***) Specimens of *Tylospira coronata* (Struthiolariidae): `P135697e` and `P135835g`, respectively. (***J***) Specimen of *Tylospira scutulata* (Struthiolariidae), `VM989`. (***K***) Specimen of *Tenagodus anguinus* (Siliquariidae), `P325996-4`. (***L***) Specimen of *Struthioptera camachoi* (Aporrhaidae), `WM15706`.

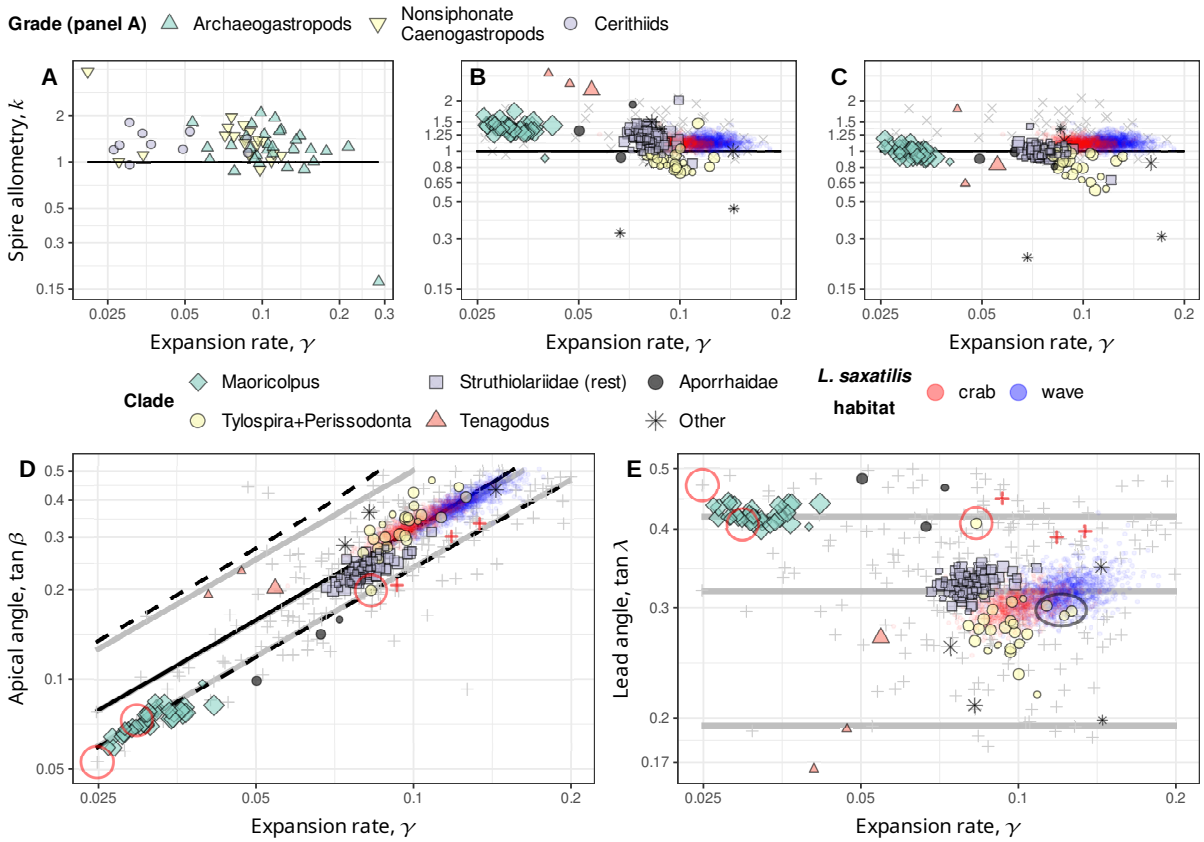

Figure 3 : Empirically observed covariation in coiling parameters. (***A***) Spire allometry, k, for Schindel's (1990) gastropod taxa, divided among his three "grades". With the notable, but unsurprising, exceptions of *Haliotis* and *Truncatella*, scatter is between $k = 1$ ($z \propto r$; isometry; solid black) and $k = 2$ ($z \propto r^2$; doming). (***B***) Same for the reanalysis of Collins et al. (2021a), where radial and longitudinal expansion rates, γ and γk, were obtained from slopes of the linear models $\log(r) \sim \theta$ and $\log(y + \text{offset}) \sim \theta$, respectively. Size of symbols represents specimen's sample size (number of measured apertures in the ontogenetic sequence; Fig. 2), which varies between 4 and 18, with median of 6. Most notable outliers are shells of the open-coiled *Tenagodus*. Scatter in k-values is similar to that in Schindel's data (here, in gray, for reference). Also shown are k-values from data of Larsson et al. (2020) on *Littorina saxatilis* (ratios of their g_h and g_w), divided between the two habitat types, crab-predation- or wave-dominated (negative or positive habitat PC1 score, respectively, in their dataset; Larsson & Butlin 2019). (***C***) As in previous panel, but values of γ and γk are now obtained from nonlinear models on untransformed response variables. Once the longitudinal starting-point problem is circumvented, scatter is closer to isometry ($k = 1$; solid black line). (***D***) Relationship between apical angle, $\tan\beta$ (in Raup's terms, $1/T$), and expansion rate, γ. Marine species from Noshita et al.'s data are presented in gray. Values for *L. saxatilis* from Larsson et al.'s data are presented according to habitat, and obtained from estimated aperture centroids (see Materials and Methods and SI). $\tan\beta$-values for Collins et al.'s data are from $y\ r$ type II major-axis regression (PCA) for aperture centroids (conical envelopes in Fig. 2). Values for *Turritella rubescens* and *T. fortilirata* from Noshita et al. (circled red on left) coincide well with the scatter for *Maoricolpus*. Thus, confirming the conversion of Noshita et al.'s T-values, as described in Materials and Methods. For comparison with Larsson et al., values for *Littorina undulata*, *L. littorea*, and *L. zebra*, from Noshita et al., are highlighted (+; left to right, respectively). Solid black line indicates Raup's (1966) whorl-overlap boundary that separates tightly-coiled and open-coiled shells of circular aperture. The fit is not bad, given that actual apertures are not circular. The boundary can be modified for other aperture shapes (lower dashed line for high-spired *Maoricolpus*) and for open umbilici (upper dashed line for *Tenagodus*; Eq.[S15] in SI). The single specimen of the recent species *Tylospira scutulata* (Fig. 2J) is highlighted (circled red in center), showing its more fusiform shape, compared to fossil *Tylospira*. Accordingly, it lies on the boundary curve for high-spired Turritellidae. Such boundary curves for tight-coiling, however, are practically indistinguishable from relationships that fixed lead angles in Eq.[2] dictate (gray lines). (***E***) Estimates of lead angle, $\tan\lambda$. Obtained from aperture centroids by regressing y on arc length, in the Collins et al. dataset (see SI). Gray lines represent median values of $\tan\lambda$ for *Maoricolpus* (upper) and *Tenagodus* (lower) and $\tan\lambda = 1/\pi$ (corresponding to Raup's whorl-overlap condition). $\tan\lambda$-estimates for specimens from Noshita et al. (gray) and Larsson et al.'s (blue or red, according to habitat) were obtained from Eq.[2]. Circled and highlighted specimens, as in the previous panel. Additionally, the ancestral forms of the *Tylospira* clade (*Perissodonta* and *T. glomerata*; Collins et al. 2021b), are circled in a black ellipse, showing their faster expansion rates, and intermediate lead angles.